AD-A094 147 CATHOLIC UNIV OF AMERICA WASHINGTON DC DEPT OF PHYSICS F/G 20/1
RESONANCES IN ACOUSTIC BOTTOM REFLECTION AND THEIR RELATION TO --ETC(U)
JAN 81 W R HOOVER, A NAGL, H UEBERALL N00014-76-C-0430

UNCLASSIFIED NL

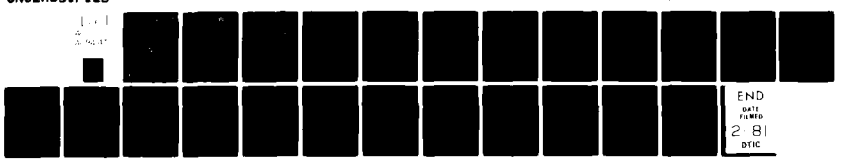

END
DATE FILMED
2 81
DTIC

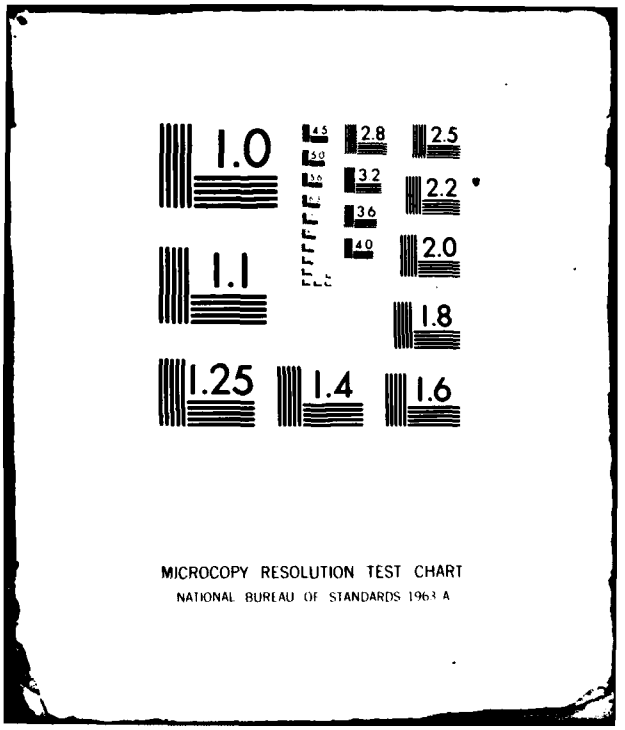
1.0
1.1
1.25
1.4
1.6
1.8
2.0
2.2
2.5
2.8
3.2
3.6
4.0
MICROCOPY RESOLUTION TEST CHART
NATIONAL BUREAU OF STANDARDS 1963 A

Resonances in Acoustic Bottom Reflectio. and their Relation to the Ocean Bottom Properties.

W. R. Hoover
David W. Taylor Naval Ship Research and Development Center
Bethesda, MD 20084

A. Nagl and H. Überall
Physics Department, Catholic University
Washington, D. C. 20064

DEPARTMENT OF PHYSICS

The Catholic University of America

Washington, D.C. 20064

LEVEL II 12

Resonances in Acoustic Bottom Reflection and their Relation to the Ocean Bottom Properties.

W. R. Hoover
David W. Taylor Naval Ship Research and Development Center
Bethesda, MD 20084

A. Nagl and H. Überall
Physics Department, Catholic University
Washington, D. C. 20064

Abstract

We have initiated a program to study the resonances in the acoustic reflection coefficient of a layered ocean bottom, patterned after the resonances of sound reflection from fluid or elastic layers[1,2]. Computer programs have been written for obtaining the reflection coefficient from multilayered fluid or elastic media, with constant or linearly depth-dependent sound velocities in each layer. Resonances are evident in the reflection coefficient both as functions of frequency and of angle of incidence, and are shown to depend on the properties of the layered ocean bottom. Results will be presented in the form of three-dimensional graphs.

Unclassified

SECURITY CLASSIFICATION OF THIS PAGE (When Data Entered)

REPORT DOCUMENTATION PAGE

1. REPORT NUMBER

2. GOVT ACCESSION NO. AD-A094-147

4. TITLE (and Subtitle) (6)

Resonances in Acoustic Bottom Reflection and their Relation to the Ocean Bottom Properties.

Techni

Feb. 1

6. PERF

7. AUTHOR(s) (10)

W. R. Hoover, A. Nagl and H. Überall (15)

8. CONT

ONR

N0001

9. PERFORMING ORGANIZATION NAME AND ADDRESS

Department of Physics (16) RR011 02

Catholic University (17) RR011080 01

Washington, DC 20064

10. PROG AREA

Program

08, Tas

Work U

11. CONTROLLING OFFICE NAME AND ADDRESS

Office of Naval Research (11) (14)

Physics Program

Arlington, VA 22217

12. REPO

Jan

13. NUM

15pp+7

14. MONITORING AGENCY NAME & ADDRESS (if different from Controlling Office)

15. SECU

U

15a. DEC SCH

16. DISTRIBUTION STATEMENT (of this Report)

Approved for public release; distribution unlimited.

17. DISTRIBUTION STATEMENT (of the abstract entered in Block 20, if different from Report)

18. SUPPLEMENTARY NOTES

19. KEY WORDS (Continue on reverse side if necessary and identify by block number)

Acoustic Reflection, Ocean Bottom, Resonances, Bottom Pr

20. ABSTRACT (Continue on reverse side if necessary and identify by block number)

We have initiated a program to study the resonances in t coefficient of a layered ocean bottom, patterned after t reflection from fluid or elastic layers . Computer prog for obtaining the reflection coefficient from multilayer media, with constant or linearly depth-dependent sound v Resonances are evident in the reflection coefficient bot frequency and of angle of incidence, and are shown to de of the layered ocean bottom. Results will be presented

DD FORM 1 JAN 73 1473 EDITION OF 1 NOV 65 IS OBSOLETE

S/N 0102-LF-014-6601

Unclas

SECURITY CLASSIFICATI

07643

Introduction

Calculated reflection coefficients for the reflection of acoustic signals from the ocean floor exhibit in general a complicated structure consisting of more or less regular sequence of peaks and dips. A typical example[3] is provided by Fig. 1 which shows the bottom reflection loss versus grazing angle for a 518-m-thick turbidite layer of 20 Hz.

Features as these can usually be attributed to resonance phenomena of some sort, and it is often found that the resonance structure, i.e. the distribution and widths of the resonance peaks, contains all relevant information about the interacting medium involved. Thus it appears logical to use knowledge about the resonance structure obtained from measurements to gain access to properties of the interacting medium, i.e. to solve the inverse scattering problem or the inverse reflection problem, as the case may be. So far few attempts have been made to apply this approach to sound reflections from the ocean floor, where it might be providing a valuable tool for acquiring information about the structure and the properties of the reflecting medium.

We have initiated a program of systematically exploring the feasibility of applying the resonance approach to sound reflections from layered media in such a way that it can be directly used for solving the problem of ocean bottom reflections. First attempts along these lines can be found in References 1 and 2 where the cases of a liquid and an elastic layer embedded in a liquid medium were considered. Here, we would like to disucss another simple

case, somewhat more relevant to ocean bottom acoustics, that of a liquid layer embedded between two different liquids.

Realistic models of the ocean floor must of course, besides layering, also include shear wave propagation, attenuation and density and velocity gradients. The implication of these complications for the resonance formalism will be briefly discussed at the end of this investigation. An example of the effects of adding shear wave propagation e.g., is already provided in Fig. 1 where the major effect is seen to be increased absorption. Adding more realistic features to the simple model we are presenting here will of course considerably increase the complexity of the analysis and the number of parameters to be dealt with. However, as will be shown, there is sufficient redundance in the information provided by the resonance analysis in our example that it can be expected that more realistic cases can also be treated satisfactorily.

Resonance Theory for the Three Fluid Case

The example chosen here for demonstrating the application of the resonance formalism is that of a liquid layer embedded between two different liquid, semi-infinite media, as indicated in Fig. 2. The reflection coefficient for this case is given by Brekhovskikh[4] and can be rewritten in the form

$$R = \frac{A\cos\delta - i(1-\tau^2)\sin\delta}{S\cos\delta - i(1+\tau^2)\sin\delta}, \qquad (1$$

with

$$A = (z_2 - z_1)/z_2 , \qquad S = (z_2 + z_1)/z_2 , \tag{2a}$$

$$\tau^2 = z_1 z_3 / z_2^2 , \qquad \delta = (2\pi f d / c_2) \cos\theta_2 \tag{2b}$$

where

$$z_i = c_i \rho_i / \cos\theta_i \tag{3}$$

are the layer impedances expressed in terms of the sound speeds c_i and the densities ρ_i. It is assumed here that $z_1 > z_2 > z_3$, which corresponds to the case of a sediment layer embedded between the ocean and a high density substratum. The parameters chosen are c_3 = 1500 m/s, c_2 = 2544 m/s, c_1 = 5495 m/s ρ_3 = 1 g/cm^3, ρ_2 = 2.2 g/cm^3, ρ_1 = 2.6 g/cm^3.

If the square of the reflection coefficient is plotted in a three-dimensional graph simultaneously vs. the frequency-thickness product fd and the incident angle θ_3 one obtains a surface, parts of which are shown in Figs. 3 through 5. The surface is seen to consist of a series of ridges and valleys which run almost parallel to the θ_3-axis for low frequency-thickness products and curve away more and more from the θ_3- axis as the value of fd is increased.

For constant θ_3 one observes a regular sequence of maxima and minima. For constant frequency-thickness products there is little structure as a function of angle for values of fd$\lesssim$5KHz-m. At around 5 KHz-m the first minimum appears (Fig. 3) and from then on the increasing curvature of the ridges and valleys leads to a growing number of maxima and minima of $|R|^2$ along lines of constant fd (Fig. 4).

Fig. 5 shows the surface of Fig. 4, covering the range of fd between 20 and 25 kHz-m, plotted upside down (thus actually showing the square of the transmission coefficient). This clearly reveals the existence of sharp ridges reminiscent of forms describing resonance-type processes. It is therefore suggestive to interpret the transition coefficient as a series of resonances (or the reflection coefficient in terms of anti-resonances) and to apply the resonance formalism developed in other areas of physics to the problem at hand, namely the analysis of the inverse reflection problem, and thereby simplifying its solution.

The basic assumption of the resonance formalism is that in the vicinity of a resonance the amplitude for a process is described essentially by a Breit-Wigner resonance form plus some slowly varying background. Following this idea, the transmission coefficient can be expanded around the maxima and then written approximately as a sum of resonance shapes, the reflection coefficient being correspondingly represented by a sum of antiresonance shapes, obtained by expanding the exact form around its minima. The sum over the resonances (or antiresonances) is to be taken only symbolically since the expansion is assumed to be valid only in the immediate vicinity of each resonance position, but is expected to fail at large distances away from the resonances where the individual resonance shape is simply expected to approach the background. For the assumed case of $Z_3 < Z_2 < Z_1$ the minima of the reflection coefficient (1) are found to be given by the condition $\cos\delta = 0$, i.e.

$$\delta_n = (2n+1)\pi/2 , \quad n = 0, 1, 2 \ldots \tag{4}$$

Linearizing around these positions with respect to δ leads to the following resonace expression for the reflection coefficient:

$$R = \sum_n \frac{F(\delta-\delta_n) \pm i G \frac{1+\tau^2}{S}}{\delta-\delta_n \pm i \frac{1+\tau^2}{S}} \tag{5}$$

with

$$F = \frac{A}{S} = \frac{z_1 - z_3}{z_1 + z_3}, \qquad G = \frac{1-\tau^2}{1+\tau^2}. \tag{6}$$

Interpreting $\frac{1+\tau^2}{S}$ as the resonance halfwidth, the expressions in the denominators of (5) are recognized as the standard resonance denominators leading to the well-known Breit-Wigner resonance shapes. Using Snell's law and the definition for δ given in (2), the resonance condition (4) can be written as

$$fd\left\{n_d^2 - \sin^2\theta_3\right\}^{1/2} = (2n+1)\,c_3/4, \quad n=0,1,2\ldots \tag{7}$$

where $n_d = c_3/c_2$.

Two Types of Resonances

For the specific example chosen, the relation between the frequency-thickness variable fd and the incident angle θ_3 as given by (7) is shown in Fig. 6 for various values of n. As this figure shows, one obtains regularly spaced resonances for the variable fd at constant values for the angle θ_3, and, if the frequency-thickness product is held constant, irregularly spaced resonances as a function of angle (indicated in Fig. 6 by circles for a few values of fd). For a more detailed discussion of the two types of resonances identified above, it is convenient to introduce new variables. For the case of the frequency-thickness resonances the reflection coefficient is rewritten as

$$R = \sum_m \frac{F(x-x_m) \pm \frac{1}{2} i G \Gamma_m}{x - x_m \pm \frac{1}{2} i \Gamma_m} \quad , \tag{8}$$

where the definitions $x = 2\pi fd/c_3$,

$$x_m = \delta_m / (n_d^2 - \sin^2\theta_3)^{1/2} \tag{9}$$

and

$$\tfrac{1}{2}\Gamma_m = (1+\tau^2) / \{ S (n_d^2 - \sin^2\theta_3)^{1/2} \} \tag{10}$$

for the amplitudes and the half-widths were used.

One thus finds that the width of the fd- resonances is independent of the order n but that it depends on the angle θ_3, being largest at normal incidence and decreasing with angle. The spacing of the resonances

$$\Delta x = \pi / (n_d^2 - \sin^2\theta_3)^{1/2} \tag{11}$$

is found to increase with angle.

For the square of the reflection coefficient one obtains

$$|R|^2 = \sum_m \frac{F^2(x-x_m)^2 + G^2\Gamma^2/4}{(x-x_m)^2 + \Gamma^2/4} \quad . \tag{12}$$

Fig. 7 compares the prediction of the resonance approximation (12) with the exact expression for $|R|^2$ obtained by squaring Eq. (1). It is seen that the agreement is excellent in the vicinity of the resonances and that the approximation fails as expected between the resonances.

The angular resonances are conveniently discussed in terms of the variable

$$y = \sin\theta_3 = \{n_d^2 - (\delta/x)^2\}^{1/2} , \tag{13a}$$

according to which the resonance positions are obtained as

$$y_m = \{n_d^2 - (\delta_m/x)^2\}^{1/2} . \tag{13b}$$

For $\cos\delta$ one obtains in the vicinity of y_m the expansion

$$\cos\delta = \cos\delta_m + (y-y_m)\{d\cos\delta/dy\}_{y=y_m} \tag{13c}$$

$$= -(y-y_m)x^2 y_m/\delta_m . \tag{13d}$$

The reflection coefficient can thus be written as

$$R = \sum_m \frac{F(y-y_m) - \frac{1}{2}iG\gamma_m}{y-y_m-\frac{1}{2}i\gamma_m} , \tag{14}$$

where the definition

$$\tfrac{1}{2}\gamma_m = (1+\tau^2)/\{S x y_m (n_d^2-y_m^2)^{1/2}\} \tag{15}$$

for the halfwidth was used.

The comparison of $|R|^2$ obtained from Eq. (14) with the exact result is shown in Fig. 8 for fd=const=50 kHz-m. Again the agreement in the vicinity of the resonances is excellent.

Relation between Resonance Parameters and Layer Parameters

The importance of the resonance approximation lies in the fact that it facilitates solving the inverse scattering problem. The quantities characterizing the resonances (positions and widths) can, in principle at least, be easily measured. On the other hand, the theoretical expressions relating these quantities to the parameters characterizing the reflecting layers are known (explicit expressions will be given below). Hence

The experimentally measured quantities can be directly related to the properties of the reflecting medium.

By measuring the critical angle θ_{cr}, the minimum value R_m of the reflection coefficient, the spacing and width of the fd-resonances at some angle and the position and width of an angle resonance at a particular frequency, all the parameters describing the reflecting medium for the particular case considered (i.e. c_1, c_2, ρ_1, ρ_2, d) can be deduced.

By measuring the spacing

$$\Delta x = 2\pi d \Delta f / c$$

of the fd- resonances at some particular angle θ_3 one obtains the ratio of sound velocities,

$$n_d = c_3/c_2 = \left\{ (c_3/2\pi d \Delta f)^2 + \sin^2\theta_3 \right\}^{1/2}. \qquad (16a$$

On the other hand, measuring the position Y_m of an angle resonance at a particular frequency f yields

$$n_d^2 = y_m^2 + (\delta_m/x)^2 \qquad (16b$$

or

$$(n_d^2 - y_m^2)^{1/2} = (2m+1)\, c_3/4fd, \qquad (17a$$

because of

$$\delta_m = \{(2m+1)\pi/2\} \cdot \{x c_3/2\pi f d\}. \qquad (17b$$

Eqs. (16b) and (17b) can be solved for n_d (or c_2) and d. From the critical angle θ_{cr} the sound speed c_1 of medium 1 can be found:

$$c_1 = c_3 / \sin\theta_{cr} \equiv c_3 / n_r . \tag{18}$$

Measurement of the halfwidth $\Gamma/2$ of the fd-resonances at some fixed angle θ_3 yields

$$(1+\tau^2)/S = \tfrac{1}{2}\Gamma\,(n_d^2 - \sin^2\theta_3)^{1/2} . \tag{18}$$

The value of τ can e.g. be found from the minimum R_m of the reflection coefficient at θ_3:

$$\tau^2 = (1-R_m)/(1+R_m) . \tag{19}$$

All other quantities being known in Eq. (18b), this equation can thus be solved for S which yields

$$S = (Z_1+Z_3)/Z_2 = (1+\tau^2) \Big/ \left\{ \tfrac{1}{2}\Gamma\,(n_d^2 - \sin^2\theta_3)^{1/2} \right\} . \tag{20}$$

S can also be written as

$$S = \frac{Z_1+Z_3}{(Z_1 Z_3)^{1/2}}\,\tau = \left\{ (Z_1/Z_3)^{1/2} + (Z_3/Z_1)^{1/2} \right\} \tau , \tag{21}$$

which can be solved for $(Z_1/Z_3)^{1/2}$ since S and τ are known. From the definition (3) of the impedances one finds:

$$(Z_1/Z_3)^{1/2} = \rho_1^{1/2} \left(\frac{1-\sin^2\theta_3}{n_r^2 - \sin^2\theta_3} \right)^{1/4} . \tag{22}$$

Since n_r is already assumed to be known, Eq. (22) thus yields ρ_1. The density ρ_2 can then be found from the known value for τ2:

$$\tau^2 = \frac{\rho_1 \rho_3}{\rho_2} \frac{n_d^2 - \sin^2\theta_3}{\cos\theta_3 \left(n_s^2 - \sin^2\theta_3\right)^{1/2}} \quad . \tag{23}$$

For the case considered here, the information available is clearly redundant since all parameters could be deduced without involving the large amount of information contained in the angular resonance except for the position of one of these resonances. Since the positions and widths of the angular resonances vary with angle it should in principle be possible to determine a much larger set of medium parameters than the five parameters involved in the present example. Thus one can hope to be able to solve the inverse reflection problem also for more realistic cases than the one considered here.

Extension of the Resonance Approach to More Complicated Cases

Adding shear waves first to the substrate, then also to the sediment, is seen from Fig. 1 to lead each time to significant changes in the reflection coefficient. The major differences occur in the size of the coefficients. The number of resonances remains the same, but the widths and positions of the individual resonances change somewhat.

Taking absorption into account will lead esentially only to reduced magnitudes of the reflection coefficient. Above the critical angle, however, new resonances may appear which can provide additional information on the reflecting medium.

If one or more layers are added to the basic model described in Fig. 2 the simple periodicity of the reflection coefficient with frequency is no longer maintained and also the angular dependence is expected to become more complicated. Fig. 9 shows the behavior of $|R|^2$ if the fluid layer in Fig. 2 is replaced by two fluid layers, each with thickness $d/2$ and with densities of 2 and 2.3 g/cm^3, and sound speeds of 2000 and 3000 m/s, respectively, the layers arranged such that the impedance still increases with depth. It is evident that there is a considerable amount of new structure which on the one hand complicates the analysis, but which on the other hand can be exploited to yield additional information.

It is seen that the pronounced resonance structure of the reflection coefficient found in the simple model is generally maintained even after more realistic features are added so that the resonance approach presented here is in principle still applicable. The question of how to relate the resonance data in the more complicated cases to the layer paramerters is presently under investigation by us. Indications are that for a large class of cases the resonance formalism demonstrated here on a simple example is indeed a promising tool for identifying ocean bottom properties, provided reflectivity measurements over a wide enough angle and frequency range are available.

Acknowledgements

Support of the Office of Naval Research, Code 421, is acknowledged.

References

1. R. Fiorito and H. Überall, JASA 65, 9 (1979).

2. R. Fiorito, W. Madigosky and H. Überall, JASA 66, 1857 (1979).

3. P. J. Vidmar and T. L. Foreman, JASA 66, 1830 (1979).

4. L. M. Brekhovskikh, Waves in Layered Media, Academic Press, New York (1960).

Figure Captions

Fig. 1. Reflection loss versus grazing angle for a 518-m-thick hypothetical turbidite layer at 20 Hz.[3]

Fig. 2. Fluid layer embedded bewteen two different fluids with incident and transmited sound wave.

Fig. 3. Square of reflection coefficient for the 3-liquid case, plotted as function of the frequency-thickness product fd between 5 and 10 kHz-m and incident angle ($0^{\circ} \leq \theta_3 \leq 20^{\circ}$).

Fig. 4. Square of reflection coefficient for the 3-liquid case, plotted as function of the frequency-thickness product fd between 20 and 25 kHz-m and incident angle ($0^{\circ} \leq \theta_3 \leq 20^{\circ}$).

Fig. 5. Square of transmission coefficient for the 3-liquid case, plotted as function of the frequency-thickness product fd between 20 and 25 kHz-m and incident angle ($0^{\circ} \leq \theta_3 \leq 20^{\circ}$).

Fig. 6. Resonance positions for the three-liquid case. The circles indicate the position of angle resonance for various frequency-thickness products. The curves indicating the resonance positions have not been drawn for all mode numbers n.

Fig. 7. The frequency-thickness resonances in the range between 45 and 50 kHz-m at $\theta_3 = 15^{\circ}$ obtained by the resonance approximation are compared with the exact value for $|R|^2$ (dashed line).

Fig. 8. The angle resonaces for fd = 50 kHz-m obtained by the resonance approximation (full lines) are compared with the exact value for $|R|^2$ (dashed line).

Fig. 9. Square of reflection coefficient for the 4-liquid case plotted as function of the frequency-thickness product fd between 20 and 25 kHz-m and incident angle ($0^{\circ} \leq \theta_3 \leq 15^{\circ}$).

Fig. 1

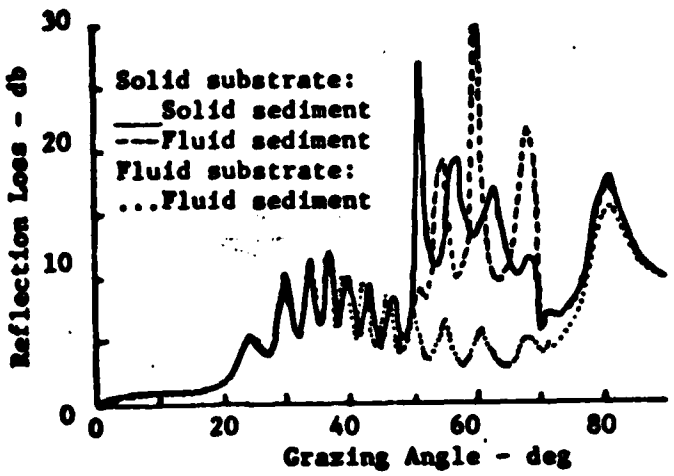
Reflection Loss - db
30
20
10
0
0
20
40
60
80
Grazing Angle - deg
Solid substrate:
Solid sediment
Fluid sediment
Fluid substrate:
...Fluid sediment

Fig. 2

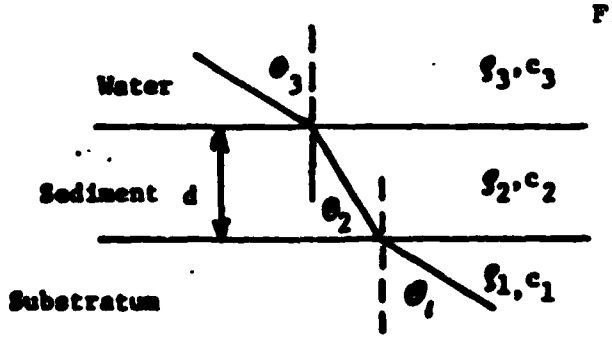
Water
θ_3
ρ_3, c_3
Sediment d
θ_2
ρ_2, c_2
Substratum
θ_1
ρ_1, c_1

Fig. 3

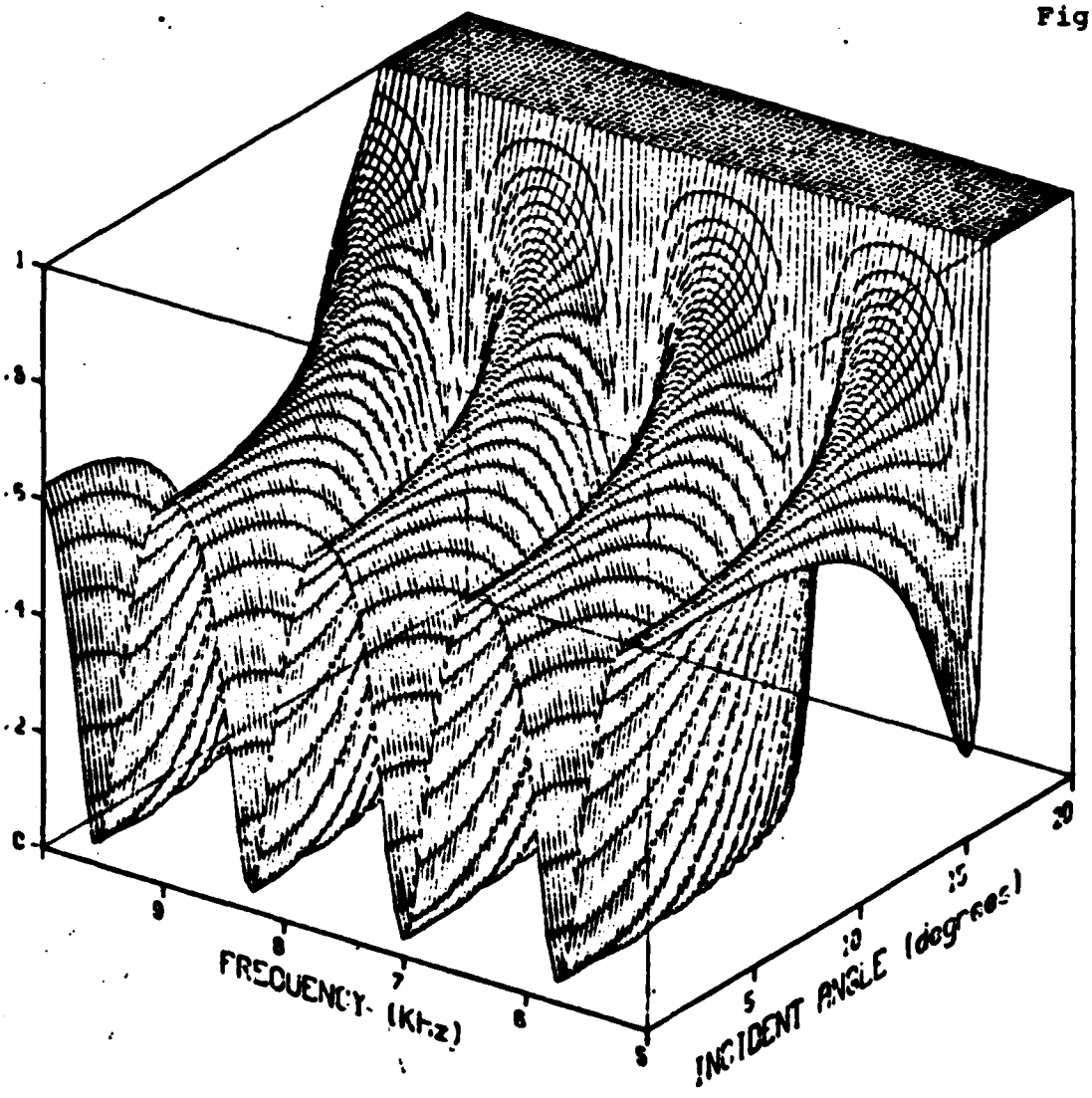
1
.8
.6
.4
.2
0
9
8
7
6
5
FREQUENCY (KHz)
5
10
15
20
INCIDENT ANGLE (degrees)

Fig. 4

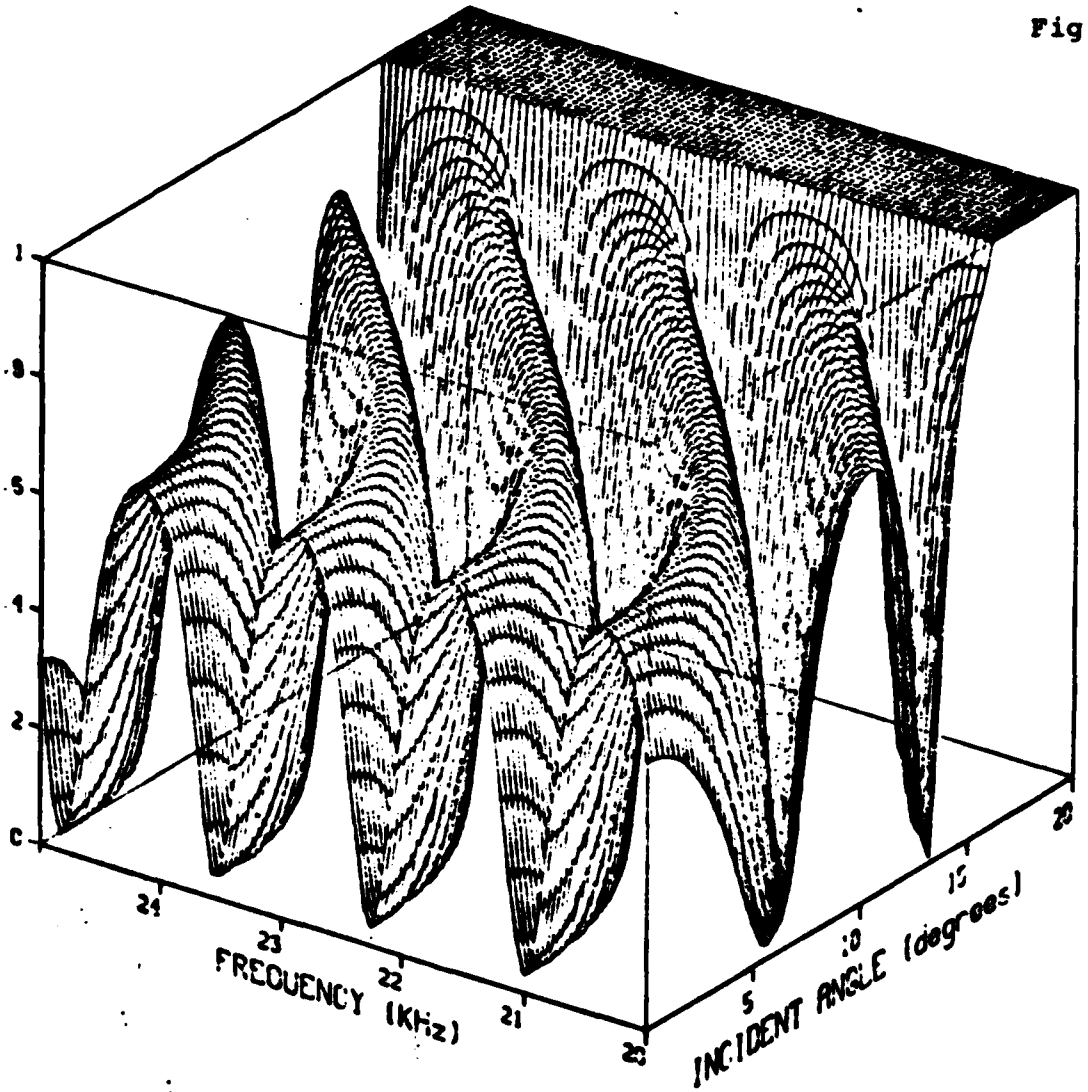
1
.8
.6
.4
.2
0
24
23
22
21
20
FREQUENCY (KHz)
5
10
15
20
INCIDENT ANGLE (degrees)

Fig. 5

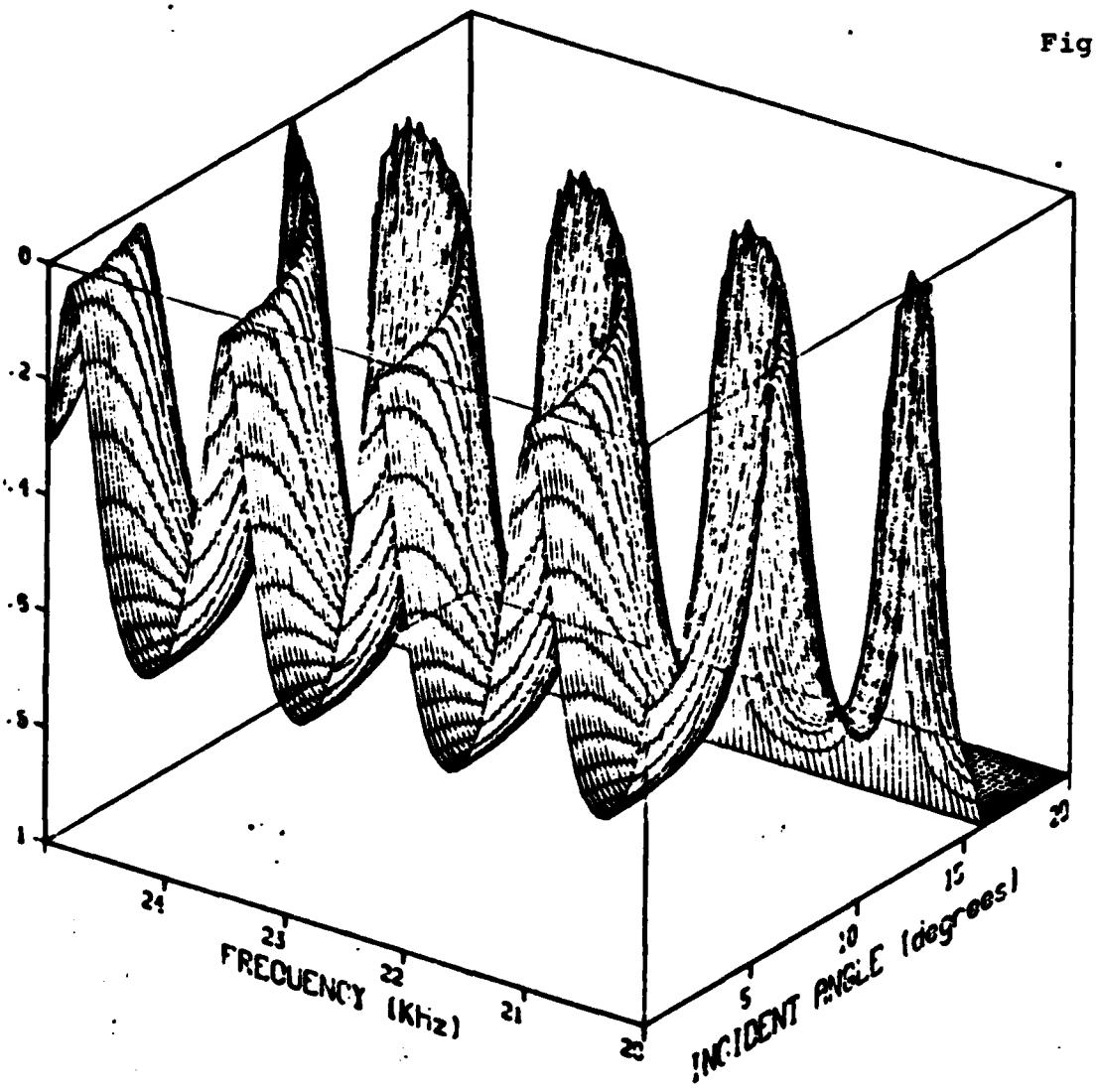
0
-2
-4
-6
-8
-10
24
23
22
21
20
FREQUENCY (KHz)
5
10
15
20
INCIDENT ANGLE (degrees)

Fig. 6

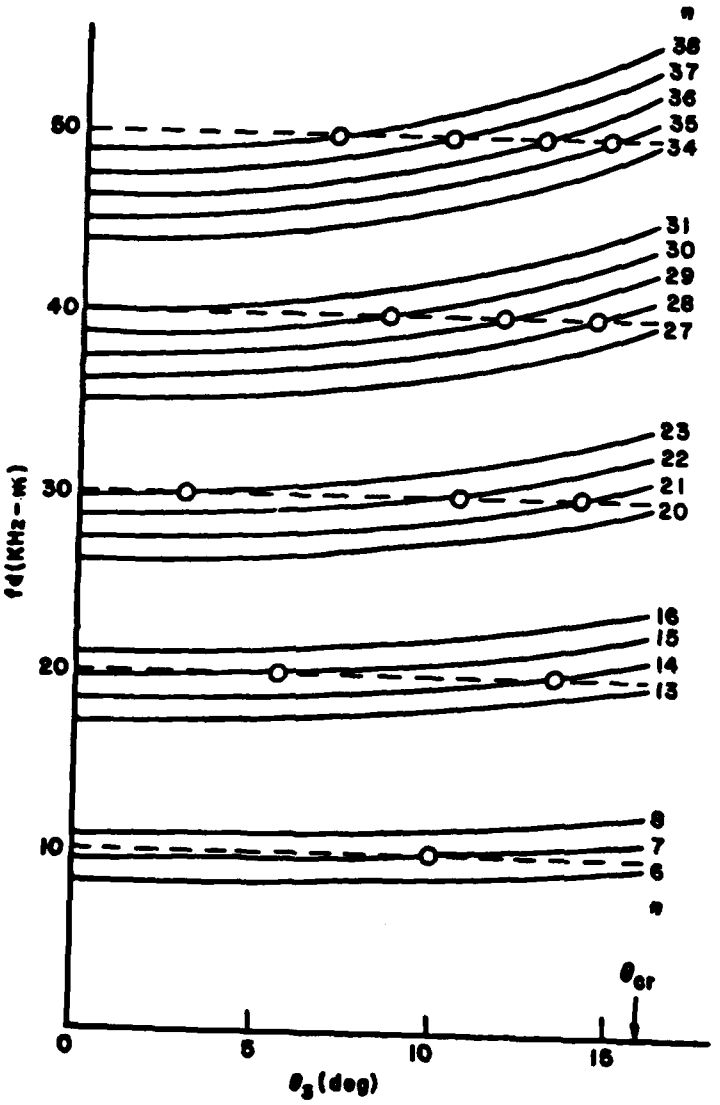
n
38
37
36
35
34
31
30
29
28
27
23
22
21
20
16
15
14
13
8
7
6
n
50
40
30
20
10
fd(KHz-m)
0
5
10
15
θ_{er}
θ_s(deg)

Fig. 7

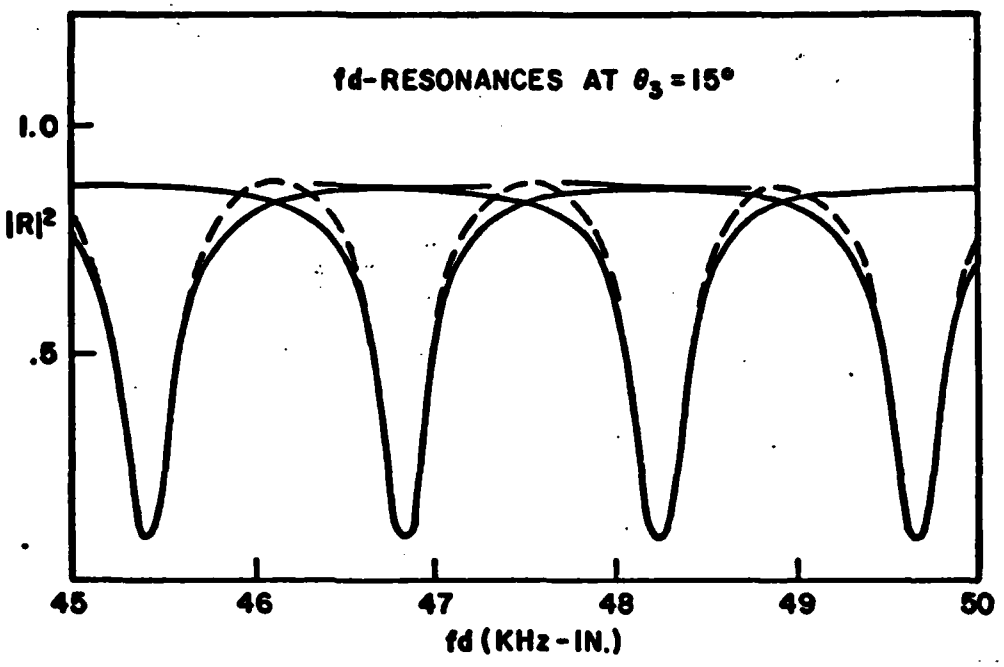
fd-RESONANCES AT $\theta_3 = 15°$
1.0
$|R|^2$
.5
45
46
47
48
49
50
fd (KHz - IN.)

Fig. 8

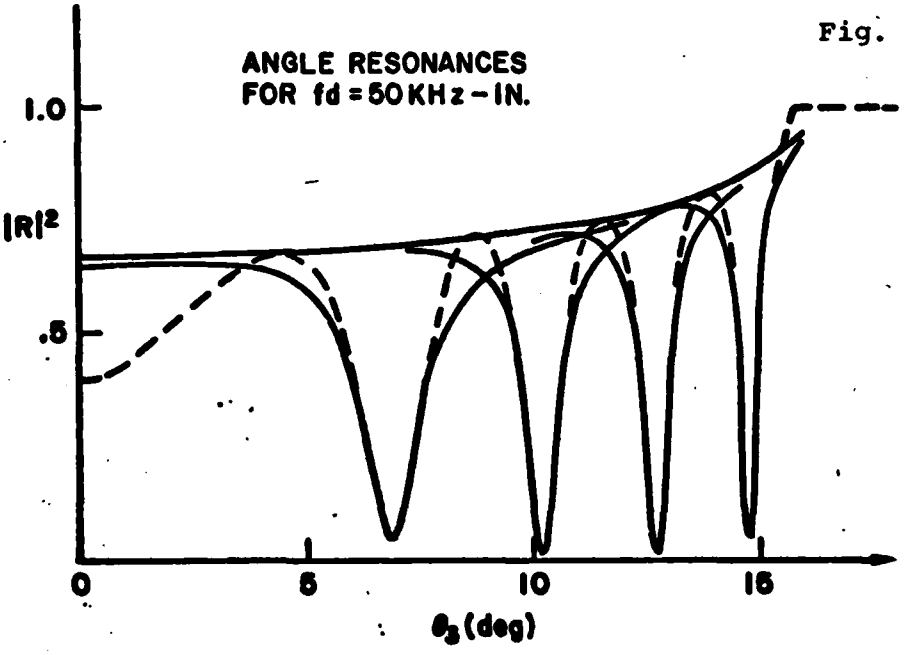
ANGLE RESONANCES
FOR fd = 50 KHz - IN.
1.0
$|R|^2$
.5
0
5
10
15
θ_3 (deg)

Fig. 9

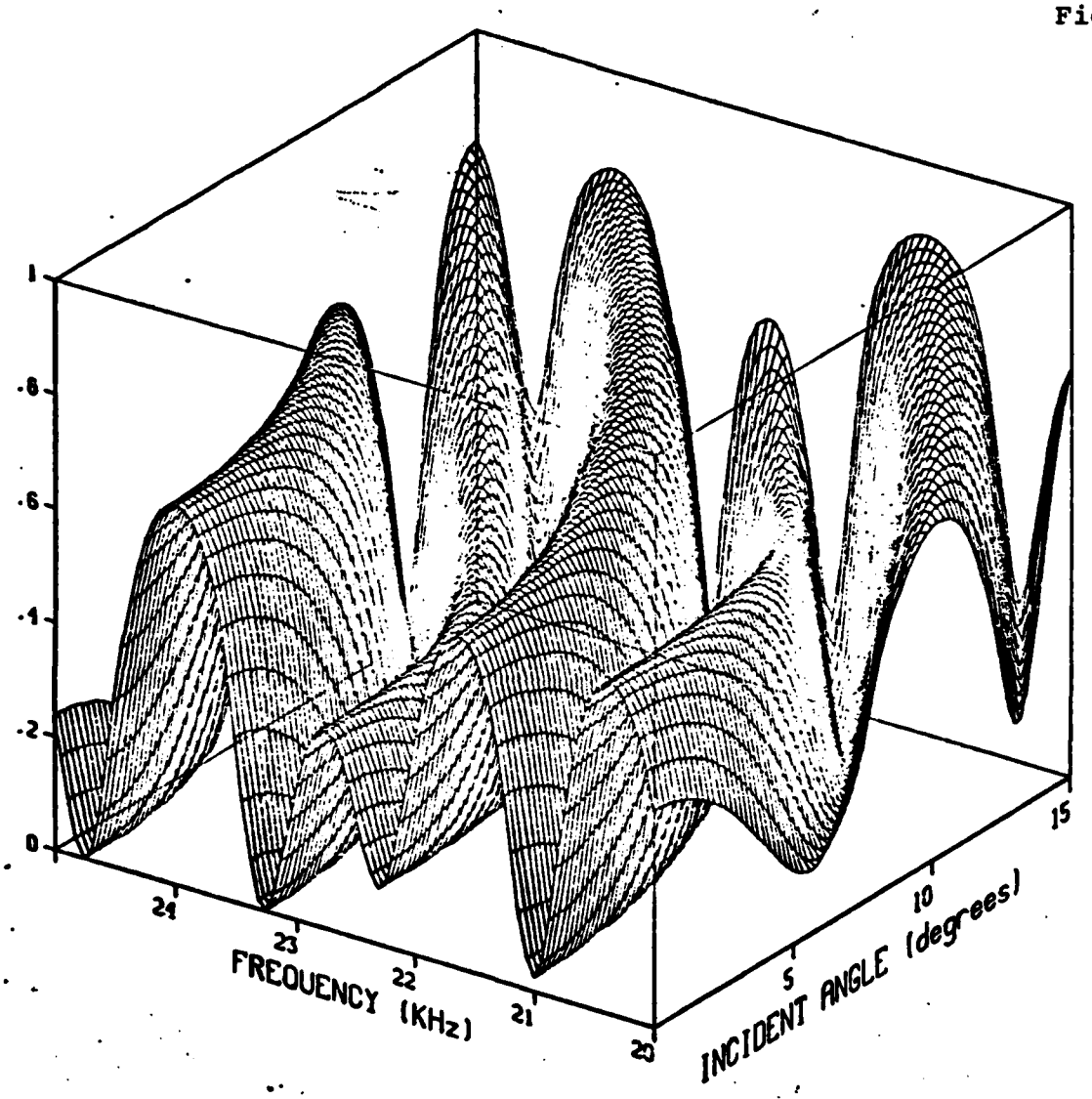
1
.8
.6
.4
.2
0
24
23
22
21
20
FREQUENCY (KHz)
5
10
15
INCIDENT ANGLE (degrees)